Journal of Applied Polymer Science

Polypropylene/Date Stone Flour Composites: Effects of Filler Contents and EBAGMA Compatibilizer on Morphology, Thermal, and Mechanical Properties

Amel Hamma,[1,2] Mustapha Kaci,[1] Alessandro Pegoretti[2]

[1]Laboratoire des Matériaux Organiques, Faculté de la Technologie, Université Abderrahmane Mira, Bejaia 06000, Algeria
[2]Department of Materials Engineering and Industrial Technologies, University of Trento, via Mesiano 77, 38123 Trento, Italy
Correspondence to: M. Kaci (E-mail: kacimu@yahoo.fr)

ABSTRACT: This work aims to study the effects of date stone flour (DSF) on morphology, thermal, and mechanical properties of polypropylene (PP) composites in the absence and presence of ethylene-butyl acrylate-glycidyl methacrylate (EBAGMA) used as the compatibilizer. DSF was added to the PP matrix at loading rates of 10, 20, 30, and 40 wt %, while the amount of compatibilizer was fixed to the half of the filler content. The study showed through scanning electron microscopy analysis that EBAGMA compatibilizer improved the dispersion and the wettability of DSF in the PP matrix. Thermogravimetric analysis (TGA) indicated a slight decrease in the decomposition temperature at onset (T_{onset}) for all composite materials compared to PP matrix, whereas the thermal degradation rate was slower. Differential scanning calorimetry (DSC) data revealed that the melting temperature of PP in the composite materials remained almost unchanged. The nucleating effect of DSF was however reduced by the compatibilizer. Furthermore, the incorporation of DSF resulted in the increase of stiffness of the PP composites accompanied by a significant decrease in both the stress and strain at break. The addition of EBAGMA to PP/DSF composites improved significantly the ductility due to the elastomeric effect of EBAGMA. © 2012 Wiley Periodicals, Inc. J. Appl. Polym. Sci. 128: 4314–4321, 2013

KEYWORDS: composites; cellulose and other wood products; compatibilization; morphology; thermal properties

Received 11 August 2012; accepted 2 October 2012; published online 22 October 2012
DOI: 10.1002/app.38665

INTRODUCTION

In recent years, considerable research effort has been undertaken to develop new composite materials derived from wood filler and thermoplastic matrices due to the increase in applications of the resulting products associated with cost reduction and ecological consideration.[1–3] Cellulosic fillers are extracted from very abundant plants and they are now fast evolving as a potential alternative to traditional ones like mica, calcium carbonate, and glass for various applications.[4,5] Indeed, wood fillers offer several advantages like low density, high specific properties, nonabrasive to processing equipment, low cost, and most importantly biodegradability.[4] However, wood fillers also exhibit some undesirable characteristics such as high moisture absorption, low thermal resistance, and highly anisotropic properties.[6] In general, the functional properties of wood plastics composites depend on various factors, including those intrinsic on the components, their interactions, and the processing conditions.[3] To develop such composites with good properties, it is necessary to properly compatibilize the cellulosic filler with the selected polymer matrix either by chemical treatments,[7,8] or by the use of compatibilizers, which are usually graft copolymers with maleic anhydride.[9] Moreover, coupling agents such as silanes, titanates, zirconates, and triazine compounds have been also employed with varied success to increase the filler-matrix adhesion.[10] Recently, the literature reported on the use of ethylene-butyl acrylate-glycidyl methacrylate (EBAGMA) terpolymer as a compatibilizer for wood polymer composites with polyolefin matrices, such as PP and polyethylene (PE).[11,12]

The valorization of date stone as a lignocellulosic material through the possibility of finding use in plastics composite manufacturing could open new market for what it is considered a waste material.[13] Furthermore, this natural product, derived from date fruit, is largely available in the north African countries. Although, there have been some studies on palm date tree fibers in plastics composites in the past few years,[6,14] the use of date stone flour (DSF) as reinforcement in polymeric materials has not been reported in the open scientific literature. Therefore, the aim of this work was to evaluate the morphology and the thermal and mechanical properties of polypropylene (PP) filled with DSF at various filler content ratios (10, 20, 30, and

40 wt %) in the absence and presence of EBAGMA terpolymer used as the compatibilizer for the system.

EXPERIMENTAL

Materials

The PP used is an isotactic homopolymer, provided by LATI spa (Varese, Italy) and commercialized under the trade name Moplen HP500H. The polymer has a melt flow index (MFI) of 1.8 g per 10 min (at 230°C, 2.16 kg).

The cellulosic filler was extracted from the date palm stone from the region of Biskra located in the Eastern-South of Algeria. Prior to grinding, the date palm stone was washed and air dried for several days. The particle size of the filler was less than 100 μm. The DSF was subjected to a Soxhlet reflux for 24 h using a solvent mixture of acetone/ethanol (75/25). The main constituents of DSF as determined by Van Soest and Wine method are as follows:[15] neutral detergent soluble (NDS) = 21.4 wt % corresponding to the majority of proteins, nonparietal sugars and fatty materials, cellulose = 16.62 wt %, hemicellulose = 19.35 wt %, lignin = 41.13 wt % and mineral ash = 1.5 wt %. The moisture content is 6.46 wt %.

The terpolymer of an ethylene butyl-acrylate glycidyl methacrylate (EBAGMA) was used as the compatibilizer for the system PP/DSF. It was kindly supplied by DuPont (Mechelen, Belgium) under the trade name Elvaloy PTW. EBAGMA has the following chemical composition: ethylene (66.75 wt %), butyl acrylate (28 wt %), and glycidyl methacrylate (5.25 wt %). According to the manufacturer, the main physical properties of EBAGMA are a MFI of 12 g per 10 min, a melting point of 72°C, a glass transition temperature of -55°C, a tensile stress at break of 5 MPa and an elongation at break of 950%. In any case, the amount of EBAGMA compatibilizer added to the PP/DSF blends was fixed to the half of the wood filler content.

Preparation of PP/DSF Composites

DSF was dried in an oven under vacuum at 80°C overnight, in order to reduce the humidity content to less than 3 wt %. Several composite samples based on PP, DSF, and EBAGMA were prepared by melt blending in a Rheomix 600 Thermo Haake® (Karlsruhe, Germany) internal mixer at various compositions, as reported in Table I. The processing parameters used are the following: temperature = 190°C, rotor speed = 60 rpm, and a residence time = 10 min. The composite samples obtained were cut down to pellets with an average particle size of about 5 mm using a grinder equipped with a set of rotating knifes. Prior to processing, The pellets were dried overnight under vacuum at 80°C and compression molded in a Carver® hydraulic press at 180°C to obtain films of about 200 μm of thickness. The films, from which the tensile specimens were cut according to ISO 527 1BA, were cooled for 10 min using cold water.

For comparative purposes, samples based on PP and EBAGMA (PP/C) blends were prepared at 5, 10, 15, and 20 wt % of compatibilizer under the same experimental conditions as the composite samples.

Table I. Code and Composition of Various PP/DSF Composite Formulations Used

Code	PP (wt %)	DSF (wt %)	EBAGMA (wt %)*
PP	100	0	0
PP/DSF10	90	10	0
PP/DSF20	80	20	0
PP/DSF30	70	30	0
PP/DSF40	60	40	0
PP/DSF10C$_{1/2}$	90	10	5
PP/DSF20C$_{1/2}$	80	20	10
PP/DSF30C$_{1/2}$	70	30	15
PP/DSF40C$_{1/2}$	60	40	20

*The weight of EBAGMA is taken on the basis of the half of the filler content ratio.

Characterization Techniques

The morphology of the composite samples was investigated using a Zeiss Supra 40 fieled emission scanning electron microscope (FESEM). The fracture of specimens was carried out under liquid nitrogen.

Thermogravimetric analysis (TGA) measurements were carried out using a Mettler® TOLEDO (Switzerland) MT5 thermogravimetric analyzer on specimens of 10–15 mg at a heating rate of 10°C min^{-1}. Samples were heated from room temperature up to 700°C to determine the complete thermal degradation of PP, DSF, and PP/DSF composites. All tests were performed under nitrogen atmosphere.

Samples were tested in a Mettler® TOLEDO (Switzerland) TC15 TA differential scanning calorimeter (DSC) in a nitrogen flow of 100 ml min^{-1}. Aluminum pans of 40 μl with holes were used and the sample weight was approximately 10 mg. All samples were first heated from -50°C to 200°C and then maintained for 5 min to erase their thermal histories. Samples were cooled from 200°C to -50°C, maintained for 5 min at -50°C before the second scan to 200°C. The heating and cooling were carried out with the same rate of 10°C min^{-1}. The melting and crystallization temperatures (T_m and T_c) were determined at the maximum endothermic and exothermic peaks, respectively. The heat of fusion (ΔH_m) was calculated from the peak area. The crystalline index (X_c) was determined as follows:[16]

$$X_c = \frac{\Delta H_m}{W \Delta H_{\text{ref}}} \quad (1)$$

where ΔH_m is the heat of fusion of neat PP and PP component in composite samples, ΔH_{ref} is the heat of fusion of 100% crystalline isotactic PP (ΔH_{ref} = 207 J g^{-1}) and W is the weight fraction of PP in the composites.

Uniaxial tensile tests at 23°C and 50% relative humidity were performed with an Instron® (Norwood, MA, USA) model 4502 tensile testing machine equipped with a 1 kN load cell. ISO 527-2 type 1BA specimens were tested at a crosshead speed of 0.25 mm min^{-1}. The strain was recorded by a resistance

Applied Polymer SCIENCE

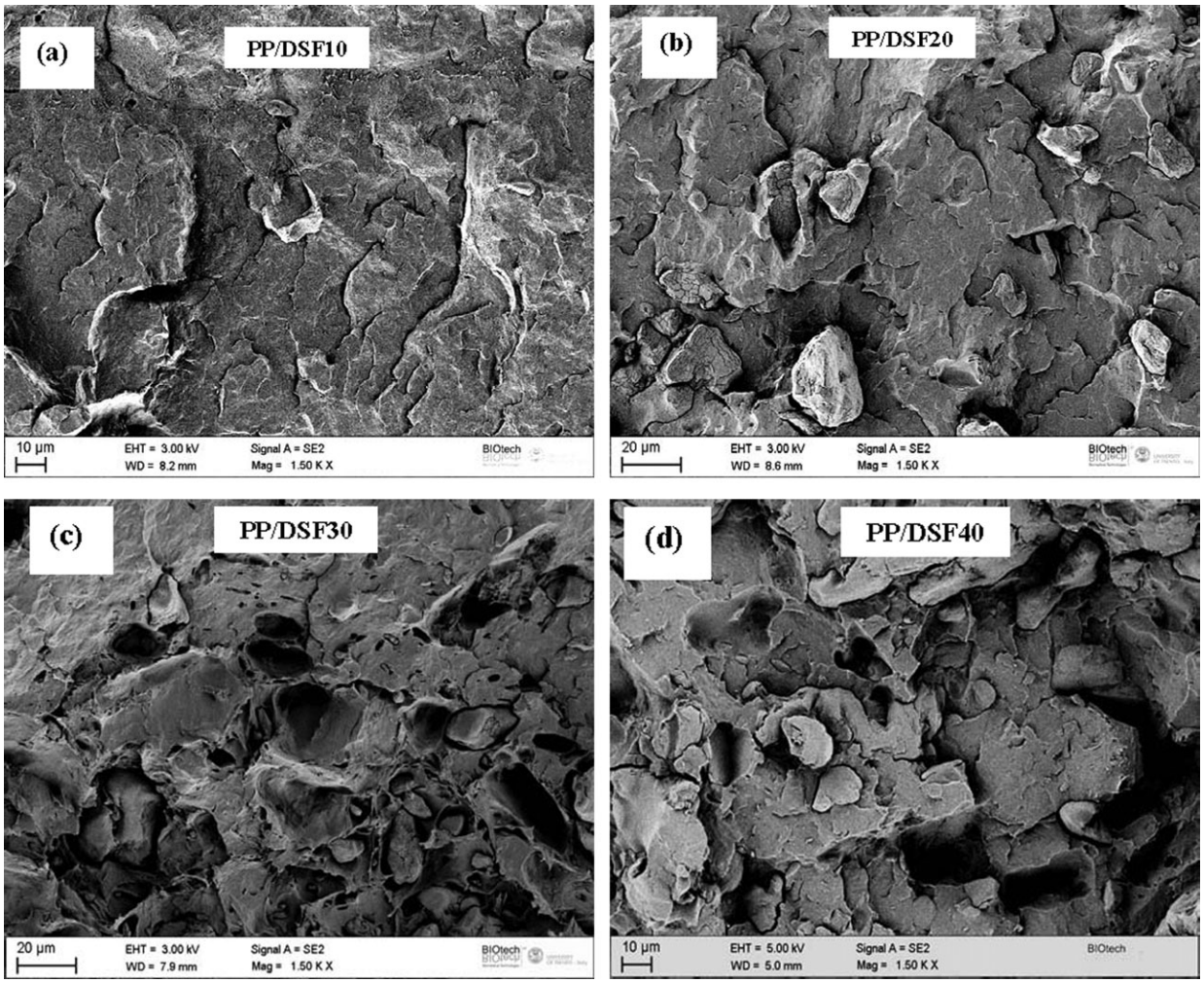

Figure 1. SEM micrographs of fracture surface of PP/DSF composites at various loading rates: (**a**): 10 wt %, (**b**): 20 wt %, (**c**): 30 wt %, and (**d**): 40 wt %.

extensometer Instron® model 2620-601 with a gage length of 12.5 mm. A maximum axial deformation of 1% was imposed during testing. According to ISO 527 standard, the elastic modulus was evaluated as secant modulus between deformation levels of 0.05% and 0.25%. Tensile tests up to fracture were performed at a higher cross-head speed (2 mm min^{-1}) and without the extensometer. For each sample, at least five specimens were tested.

Impact tests were performed by a CEAST® (Turin, Italy) impact pendulum under tensile configuration. The hammer was released from a height selected to reach an impact velocity of 2 m s^{-1} with an impact energy of 4.38 J (hammer mass of 2.191 kg). The tests were carried out at room temperature (23°C) and at least, five specimens were tested for each sample.

RESULTS AND DISCUSSION

Morphological Analysis

Figure 1(a–d) show the SEM micrographs of the fracture surface of PP/DSF composites without the EBAGMA compatibilizer at different filler content ratios, i.e., 10, 20, 30, and 40 wt %, respectively. As well expected, the SEM micrographs show that the addition of DSF in the PP matrix results in a phase separation morphology characterized by the formation of DSF aggregates. The size and number of aggregates appear to increase with the filler ratios. Indeed, one can notice from Figure 1 that no interaction is developed between the PP matrix and the cellulosic filler. Furthermore, with increasing the filler content to 30 and 40 wt %, the date stone particles are pulled out from the matrix during fracture, while the surface exhibits a large number of microvoids as clearly shown in Figure 1(c) and (d). This may be explained as a result of a somewhat poor bonding strength and a weak adhesion between the filler and the PP matrix.

Figure 2(a–d) show the SEM micrographs of the fracture surface of PP/DSF composites at filler contents of 10, 20, 30, and 40 wt %, respectively, in the presence of EBAGMA compatibilizer. The SEM micrographs show that DSF is embedded in the PP matrix to a larger extent showing an intimate contact between the two components so that it is not easy to distinguish the two phases. Moreover, homogenous and regular fracture surface is observed indicating better dispersion of the cellulosic filler in the matrix, thus better interaction between the date stone particles and the

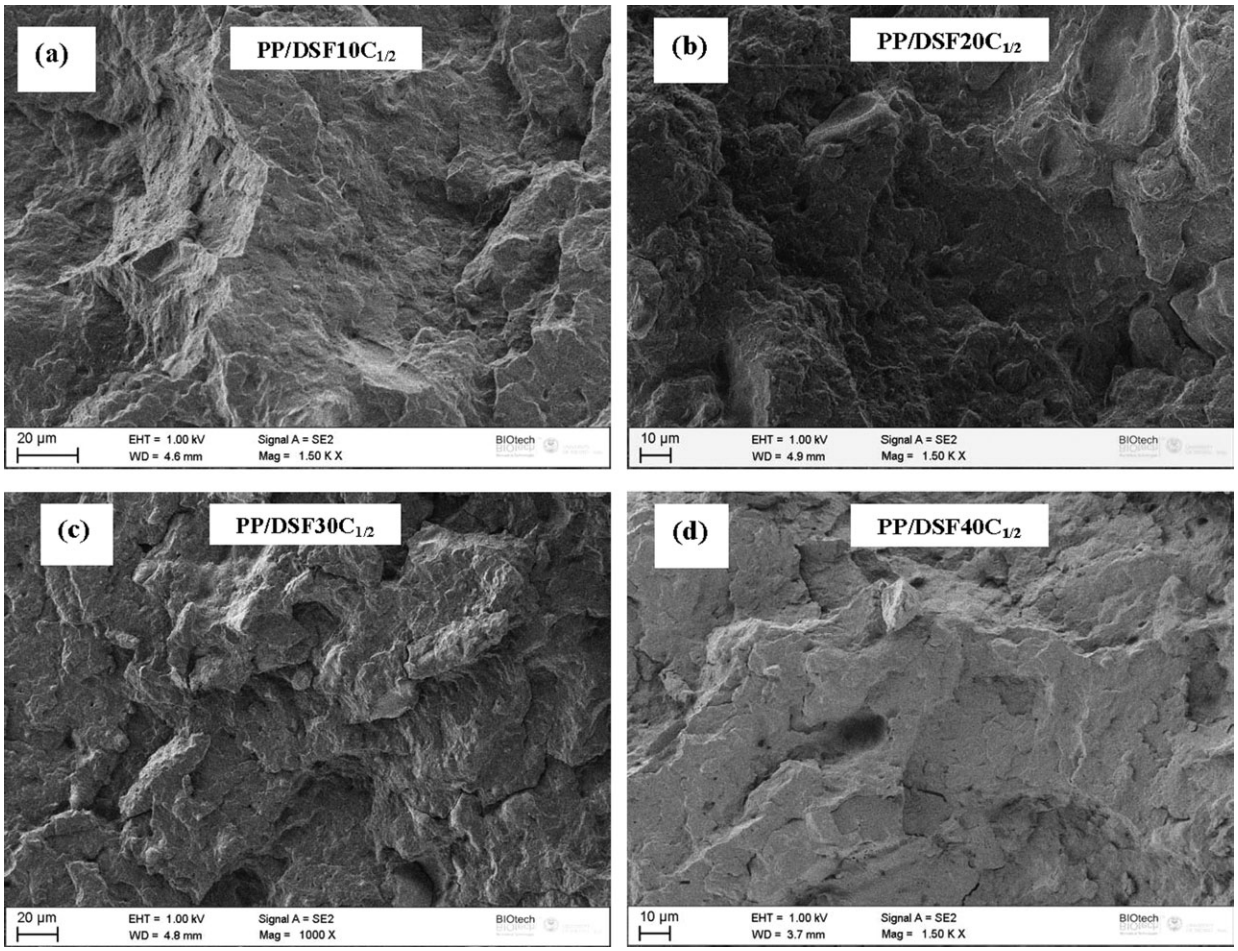

Figure 2. SEM micrographs of fracture surface of PP/DSF composites compatibilized with EBAGMA. (**a**): (90/10)/5 wt %, (**b**): (80/20)/10 wt %, (**c**): (70/30)/15 wt %, and (**d**): (60/40)/20 wt %.

PP matrix. According to the literature,[17] this behavior could be attributed to chemical interactions between the glycidyl methacrylate groups of EBAGMA compatibilizer and the hydroxyl groups of the cellulosic filler which improve the wettability of DSF and increase the interfacial adhesion between the filler and the PP matrix. This morphology seems suitable to obtain better mechanical properties in comparison with that observed for uncompatibilized composites.

Thermogravimetric Analysis

Thermal degradation is a crucial aspect in the development of wood/polymer composites since it strongly affects the selection of proper processing conditions. Furthermore, thermally induced degradation of cellulosic fillers may lead to deterioration of the mechanical properties of the polymer composites.[18,19] The TGA thermograms carried out on neat PP, DSF, EBAGMA, and the composite materials are presented in Figures 3–5.

Figure 3 shows the TGA thermogram of neat PP compared to those of DSF and EBAGMA. Accordingly, EBAGMA compatibilizer exhibits a higher thermal stability than PP matrix and DSF. Moreover, it is observed that the thermal degradation of PP occurs in the temperature range of 314–400°C and proceeds mainly by thermal scission of C–C chain bonds and hydrogen transfer at the site of scission. The thermal degradation of EBAGMA occurs between 380°C and 450°C through random

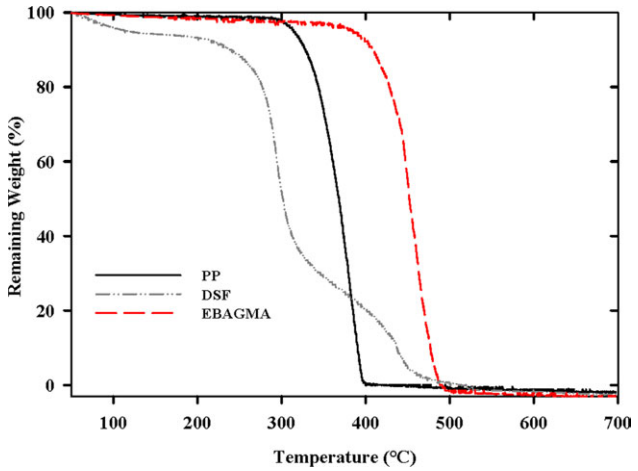

Figure 3. TGA thermograms of neat PP, DSF, and EBAGMA compatibilizer. [Color figure can be viewed in the online issue, which is available at wileyonlinelibrary.com.]

Applied Polymer SCIENCE

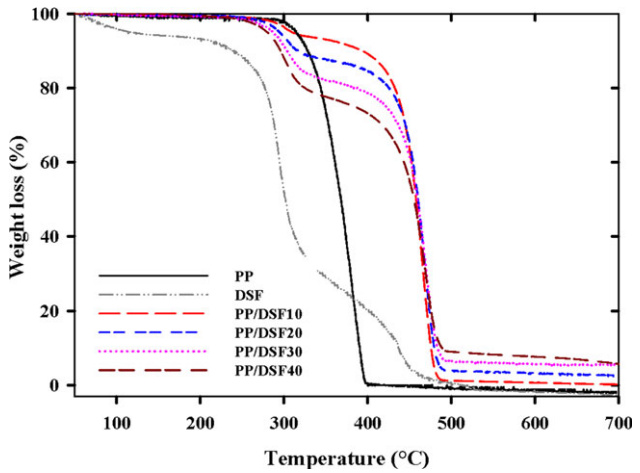

Figure 4. TGA thermograms of PP/DSF composites recorded at different loading rates, i.e., 10, 20, 30, and 40 wt % compared to neat PP and DSF. [Color figure can be viewed in the online issue, which is available at wileyonlinelibrary.com.]

chain scission and radical chain mechanisms. Both, PP and EBAGMA thermograms show single-stage decomposition with the maximum degradation rate at 386°C and 454°C, respectively. On the contrary, the TGA thermogram of DSF exhibits several decomposition steps, which start by a slight decrease in weight observed at roughly 100°C. This is attributed to the moisture content of filler. The next degradation step observed above 100°C is attributed to the hemicellulose decomposition. From 240°C, the thermal degradation of cellulose takes place by hydration and depolymerization up to 360°C resulting in the formation of volatile products and char. The major weight loss in the temperature range of 360–500°C indicates the pyrolitic degradation of lignin involving the fragmentation of interunit linkages (releasing monomeric phenols into the vapor phase), decomposition and condensation of the aromatic rings.[20,21] Figure 4 shows the TGA thermograms of uncompatibilized PP/DSF composites recorded at various loading rates, i.e., 10, 20, 30, and 40 wt % compared to neat PP and DSF. It is observed in Figure 4 that additionally to the minor weight loss occurring around 100°C due to moisture evaporation, the incorporation of DSF to the PP matrix causes a decrease in the degradation temperature at onset being much pronounced at higher filler content ratios. This is generally attributed to the lower thermal stability of the cellulosic filler as previously discussed. In contrast, the degradation rate is slower above 470°C, as a result of increased char content, which may contribute to protect the remaining composite material from further thermal degradation. The values of typical degradation temperatures of PP and PP/DSF composites at different filler content ratios are summarized in Table II. The results indicate that the values of T_{mr} and $T_{50\%}$ increased by almost 90°C and 80°C, respectively, for the whole uncompatibilized PP composites compared to neat PP. Figure 5 shows the TGA thermograms of the compatibilized PP/DSF composites recorded at 10, 20, 30, and 40 wt %. From both Figure 5 and Table II, the addition of EBAGMA in PP/DSF composites results in a slight improvement in thermal stability if we consider that the values of the degradation temperature at 10% and 50% weight loss increase by 2°C to 4°C compared to uncompatibilized ones.

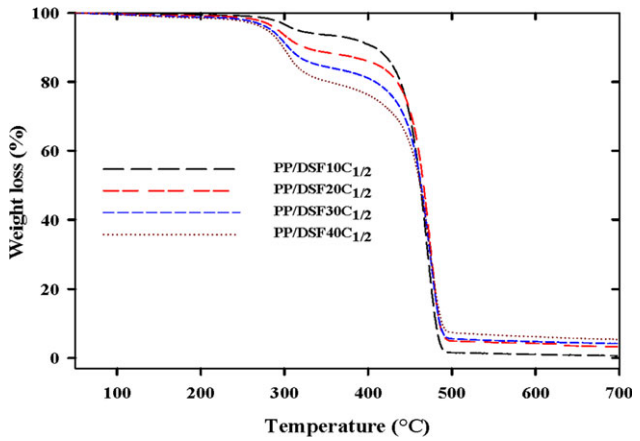

Figure 5. TGA thermograms of PP/DSF composites compatibilized with EBAGMA recorded at different loading rates, i.e., 10, 20, 30, and 40 wt %. [Color figure can be viewed in the online issue, which is available at wileyonlinelibrary.com.]

Table II. TGA Data for Neat PP and PP/DSF Composite Materials

Formulation	T_{onset} (°C)	$T_{10\%}$ (°C)	$T_{50\%}$ (°C)	$T_{max.rate}$ (°C)	Char (wt %)
PP	298	329	368	387	0
PP/DSF10	286	393	458	465	0.98
PP/DSF20	260	315	460	471	3.63
PP/DSF30	251	302	459	471	5.97
PP/DSF40	238	294	458	471	8.31
PP/DSF10$C_{1/2}$	285	406	462	471	1.29
PP/DSF20$C_{1/2}$	261	317	462	471	3.96
PP/DSF30$C_{1/2}$	251	304	463	471	5.10
PP/DSF40$C_{1/2}$	239	298	462	471	6.70

Differential Scanning Calorimetry

Melting temperature (T_m), melting enthalpy (ΔH_m), crystalline index (X_c), crystallization temperature (T_c), and crystallization enthalpy (ΔH_c) are determined from DSC thermograms and the values reported in Tables III and IV. The data in Table III indicate that T_m remains almost unchanged around 164°C for all composite materials, and its value is very close to that of neat PP (165°C). Within experimental errors, this result means that crystal thickness is not influenced consistently by the filler content ratio.[20] On the other hand, an increase in ΔH_m is observed for the uncompatibilized composites with increasing the DSF content. Similar trend is also observed for X_c indicating that DSF behaves as a nucleating agent promoting the crystallization of PP. This phenomenon is more pronounced at higher filler contents. For the compatibilized composites, the DSC data reported in Table III indicate a decrease in the values of ΔH_m and X_c. This is attributed to the inhibition effect of the compatibilizer on the polymer crystal formation when it coats the filler, thus limiting their nucleating effect on PP matrix.

Table III. Melting Properties of PP and PP/DSF Composites with and Without EBAGMA

Code	T_m (°C)	ΔH_m (J g^{-1}_{PP})	X_c (%)
PP	165	97	47
PP/DSF10	164	101	48.62
PP/DSF20	164	100	48.41
PP/DSF30	164	103	49.74
PP/DSF40	163	110	53.04
PP/DSF10$C_{1/2}$	164	99	47.76
PP/DSF20$C_{1/2}$	164	97	46.71
PP/DSF30$C_{1/2}$	164	93	44.93
PP/DSF40$C_{1/2}$	163	91	43.90

Furthermore, the addition of EBAGMA may alter the organization of PP chains due to the presence of more imperfections.[21] Table IV reports the values of crystallization temperature (T_c) and crystallization enthalpy (ΔH_c) for pure PP and PP/DSF composites in the absence and presence of EBAGMA. Furthermore, the degree of crystallization rate (ΔT_1) and the degree of supercooling (ΔT_2) were also determined. ΔT_1 is defined as the difference between T_c at onset (T_{cons}) which is the starting point of the crystallization process, and T_c; so that a small ΔT_1 value refers to a fast crystallization rate. ΔT_2 which is the degree of supercooling is defined as the difference between the melting temperature (T_m) and the crystallization temperature (T_c).[22] In this respect, the data reported in Table IV indicate that the incorporation of DSF to PP matrix leads to a decrease in the degree of supercooling (ΔT_2). According to the literature,[23,24] this result suggests that DSF particles act as heterogeneous nuclei. The heterogeneous nucleation coupled with an increase of ΔT_1 occurring at lower supercooling result in the formation of crystallites with perfect structure and bigger size. Whereas, the addition of EBAGMA compatibilizer to PP/DSF composites results in a slight decrease in ΔT_1 by a few degrees (almost 2–3°C) delaying the PP nucleation. This phenomenon is accompanied by an increase in the supercooling degree (ΔT_2) producing less perfect structure, which implies lower structure stability. This may be explained as a result of strong interactions occurring between EBAGMA and DSF which restrict the mobility and subsequently reduce the crystallization ability of PP chains.[25]

Table IV. Crystallization Properties of PP and PP/DSF Composites with and Without EBAGMA

Code	T_c (°C)	ΔH_c (J g^{-1}_{PP})	ΔT_1* (°C)	ΔT_2** (°C)
PP	116	92	2.95	48.84
PP/DSF10	116	95	3.80	48.12
PP/DSF20	117	94	3.83	47.04
PP/DSF30	117	97	3.55	47.08
PP/DSF40	116	104	3.98	47.83
PP/DSF10$C_{1/2}$	115	94	3.93	48.80
PP/DSF20$C_{1/2}$	115	93	3.69	48.42
PP/DSF30$C_{1/2}$	116	94	3.32	48.37
PP/DSF40$C_{1/2}$	116	94	3.20	47.35

*ΔT_1: is degree of crystallization rate ($T_{c\ onset} - T_c$)
**ΔT_2: is degree of supercooling ($T_m - T_c$)

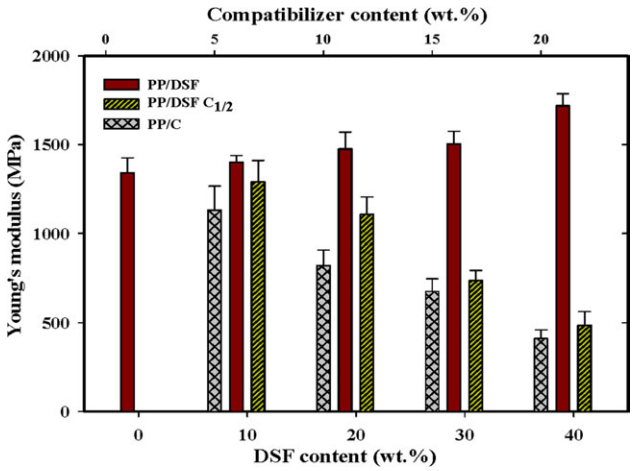

Figure 6. Young's modulus as a function of DSF content for uncompatibilized and EBAGMA compatibilized PP/DSF composites. [Color figure can be viewed in the online issue, which is available at wileyonlinelibrary.com.]

Tensile Measurements

Figures 6–8 show the variation of tensile properties of neat PP and PP/DSF composites with and without EBAGMA compatibilizer. Furthermore, the tensile properties of PP/EBAGMA (*C*) blends are also measured and compared to the compatibilized composites. Figure 6 shows the variation of Young's modulus (*E*) as a function of DSF content ratios. It is observed a progressive increase in Young's modulus with increasing the amount of DSF. Indeed, the *E*-value for neat PP is roughly 1340 MPa. This value increases by almost 10% with adding 10 wt % of DSF. With further increase of the filler content to 40 wt %, the modulus increases by almost 30%. This result is consistent with the

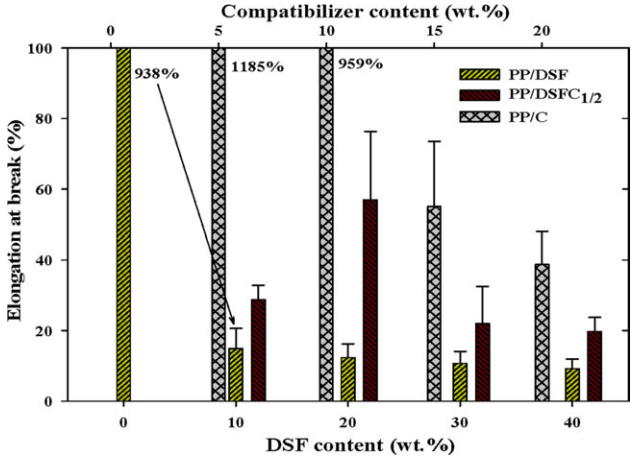

Figure 7. Elongation at break as a function of DSF contents for uncompatibilized and EBAGMA compatibilized PP/DSF composites. [Color figure can be viewed in the online issue, which is available at wileyonlinelibrary.com.]

Applied Polymer SCIENCE

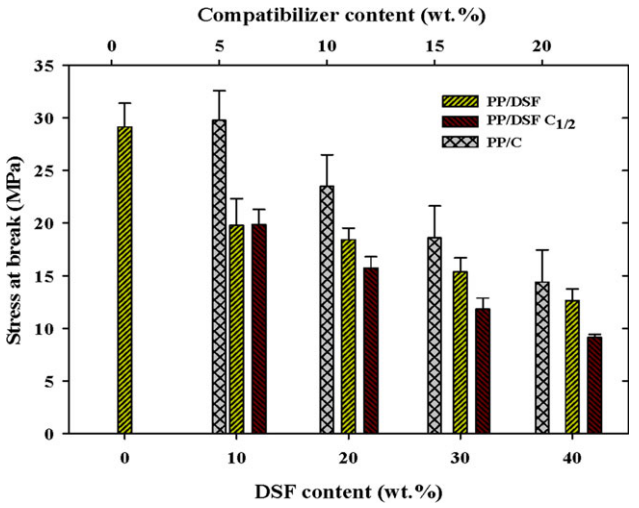

Figure 8. Stress at break as a function of DSF content for uncompatibilized and EBAGMA compatibilized PP/DSF composites. [Color figure can be viewed in the online issue, which is available at wileyonlinelibrary.com.]

literature data.[25] As a matter of fact; wood particles exert the expected reinforcing effect leading to an increase in stiffness.

Elongation at break and stress at break for the uncompatibilized PP/DSF composites are presented in Figures 7 and 8, respectively. Both properties exhibit a decrease with the addition of DSF compared to neat PP. For instance, the addition of 10 wt % of DSF to PP matrix induces a reduction in elongation at break by almost 98% compared to neat PP, while the stress at break decreases by 32%. According to the literature,[26,27] when the filler particles are added to the polymer matrix, there is an enhancement of stiffness of the composite materials restricting the matrix deformation and the plasticity domain. The weak interfacial area between the filler and the matrix increases due to the lack of intimate adhesion and poor interactions between the composite components, which consequently lead to decrease the tensile strength. These results are consistent with those obtained by SEM analysis from which it was reported that an increase in the filler content yields to the formation of more defects (microvoids) in the PP matrix. In addition, the presence of hydroxyl groups in DSF is another factor responsible for the repulsive character toward PP matrix. However, the incorporation of EBAGMA in the PP composites reduces the stiffness. The Young's modulus of the compatibilized composite materials decreases by almost 19, 34, 40, and 57% corresponding respectively to 10, 20, 30, and 40 wt % loading rates, compared to uncompatibilized ones. This behavior can be attributed to the lower modulus of EBAGMA which behaves as an impact modifier.[11] According to Pracella et al.[1] and Wang et al.,[28] the tensile modulus of composites as well as the tensile strength are dependent on the structure and type of the compatibilizer used. The authors reported that the use of an elastomeric one induces to a plasticizing effect and subsequently, a decrease in both modulus and strength. To confirm whether or not the compatibilizer affects strongly the modulus of the PP matrix, binary blends of PP and EBAGMA (PP/C) have been prepared in the same proportions as those used in compatibilized composites. The results indicate a decrease in the values of modulus up on adding EBAGMA to PP matrix. Specifically, the Young's modulus decreases by almost 16% for 5% of EBAGMA. With a further increase in the compatibilizer ratio, the *E*-values are significantly reduced by 38.7, 49.6, and 69.3% for blends containing 10, 15, and 20% of compatibilizer, respectively. Similar effect is also observed for the compatibilized PP/DSF composites compared to uncompatibilized samples. The stress at break displays also lower values in the presence of EBAGMA and the decrease in this property is estimated to roughly 12, 21, and 29% for 20, 30, and 40 wt % loading ratios, respectively. The decrease in stress at break is also observed for the binary blends (PP/C) which may be explained by the elastomeric character of EBAGMA. On the other hand, the addition of EBAGMA results in a positive effect on the elongation at break which is significantly improved for all PP/DSF composites compared to uncompatibilized ones. The compatibilized PP composite filled at 20 wt % show the highest improvement, exhibiting more than 300% increase. This may be due to the development of a flexible interphase around the DSF particles as reported by some authors.[28–31]

Impact Strength

The variation of impact strength (IS) as a function of filler content for the neat PP and PP/DSF composites with and without EBAGMA is shown in Figure 9. It is observed that IS of PP/DSF composites decreases considerably as the DSF content ratio is increasing. Specifically, the IS of the composite materials decreases by roughly 53, 66, 72, and 81% corresponding to the filler content ratios of 10, 20, 30, and 40 wt %, respectively. This finding has also been reported by Karmarkar et al.[4] and it is attributed to lower filler dispersion and poor filler–matrix interaction. This behavior is consistent with morphological data. The formation of agglomerates and other defects are responsible for the mechanical failure of the composite materials through propagation of the microcracks during impact acting as stress concentrators.[26,32] The addition of EBAGMA results in the improvement of the IS for all PP composites as shown in Figure 9. In fact, IS shows a percent increase of almost 14, 29,

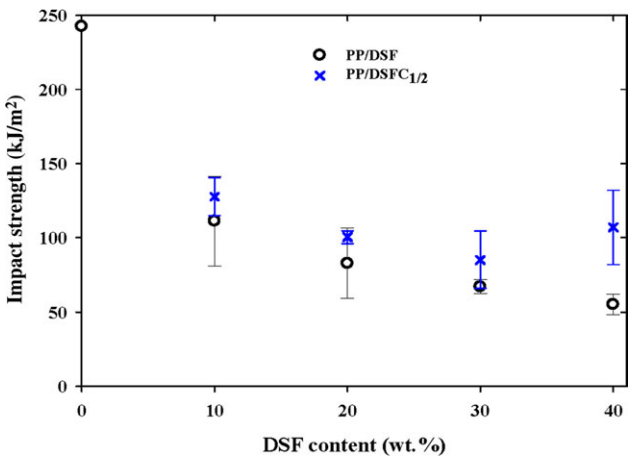

Figure 9. IS as a function of DSF content for neat PP and PP/DSF composites without and with EBAGMA compatibilizer. [Color figure can be viewed in the online issue, which is available at wileyonlinelibrary.com.]

37, and 94 corresponding respectively to the composite materials filled with 10, 20, 30, and 40 wt % compared to the uncompatibilized composites. The enhancement of IS is interpreted as an improvement of the interfacial adhesion between the composite components resulting in more efficient stress transfer from the polymer matrix to the filler.[11] Thus, the compatibilized composites are able to absorb higher amount of energy to stop crack propagation.[33,34] There is also another explanation for the improvement of IS which is related to the nature of EBAGMA through butyl acrylate group, which acts as an impact modifier.[35]

CONCLUSIONS

In this work, composite materials based on PP and DSF were prepared at various filler content ratios (10, 20, 30, and 40 wt %) in the absence and presence of EBAGMA used as the compatibilizer. The SEM analysis indicated that the morphology of PP/DSF composites is improved by the EBAGMA compatibilizer. DSF is uniformly dispersed and embedded in the PP matrix independently of the loading rates. TGA data showed that the degradation rate of the PP composites was retarded above 470°C due to DSF although; the thermal stability measured at onset was slightly shortened. DSC thermograms indicated the occurrence of a nucleating effect of DSF on the crystallization of PP as evidenced by an increase in X_c of PP in the composite materials. However, the addition of EBAGMA to PP/DSF composites induces a decrease in X_c of PP due to interactions between the compatibilizer and the filler resulting in the restriction of crystallite organization. Improved elongation at break and IS were also reported up on addition of EBAGMA to PP/DSF composites in comparison to uncompatibilized ones, whereas Young's modulus and stress at break were reduced. The mechanical results confirm the role of EBAGMA as an impact modifier.

A.H. would like to thank the Averroes program for his financial support (Grant N° 1 Averroes 3) in the framework of the European program Erasmus Mundus and the hosting Department of Materials Engineering and Industrial Technologies of the University of Trento, Italy.

REFERENCES

1. Kowalczyk, M.; Piorkowska, E.; Kulpinski, P.; Pracella, M. *Compos. A* **2011**, *42*, 1509.
2. Kaci, M.; Kaid, N.; Boukerrou, A. *Comp. Interf.* **2011**, *18*, 295.
3. Bouza, R.; Marco, C.; Naffakh, M.; Barral, L.; Ellis, G. *Compos. A* **2011**, *42*, 935.
4. Karmarkar, A.; Chauhan, S. S.; Modak, J. M.; Chanda, M. *Compos. A* **2007**, *38*, 227.
5. Pandey, J. K.; Ahn, S. H.; Lee, C. S.; Mohanty, A. K.; Misra, M. *Macromol. Mater. Eng.* **2010**, *295*, 975.
6. Alawar, A.; Hamed, A.M.; Al-Kaabi, K. *Compos. B* **2009**, *40*, 601.
7. Li, X.; Tabil, L.G.; Panigrahi, S. J. *Polym. Environ.* **2007**, *15*, 25.
8. Kalia, S.; Kaith, B. S.; Kaur, I. *Polym. Eng. Sci.* **2009**, *49*, 1253.
9. Tserki, V.; Matzinos, P.; Panayiotou, C. J. *Appl. Polym. Sci.* **2003**, *88*, 1825.
10. Awal, A.; Ghosh, S. B.; Sain, M. J. *Therm. Anal. Calorim.* **2010**, *99*, 695.
11. Kaci, M.; Cimmino, S.; Silvestre, C.; Duraccio, D.; Benhamida, A.; Zaidi, L. *Macromol. Mater. Eng.* **2006**, *291*, 869.
12. Kaci, M.; Djidjelli, H.; Boukerrou, A.; Zaidi, L. *Express Polym. Lett.* **2007**, *1*, 467.
13. Kaddami, H.; Dufresne, A.; Khelifi, B., Bendahou, A.; Taourirte, M.; Raihane, M.; Issartel, N.; Sautereau, H.; Gérard, J. F.; Sami, N. *Compos. A* **2006**, *37*, 1413.
14. Al-Khanbashi, A.; Al-Kaabi, K.; Hammami, A. *Polym. Comp.* **2005**, *26*, 486.
15. Van Soest, P. J.; Wine, R. H. J. *Assoc. Office Agricul. Chem.* **1967**, *50*, 50.
16. Faria, H.; Cordeiro, N.; Belgacem, M. N.; Dufresne, A. *Macromol. Mater. Eng.* **2006**, *291*, 16.
17. Kaci, M.; Hamma, A.; Pillin, I.; Grohens, Y. *Macromol. Mater. Eng.* **2009**, *294*, 532.
18. Nuñez, A. J.; Kenny, J. M.; Reboredo, M. M.; Aranguren, M. I.; Marcovich, N. E. *Polym. Eng. Sci.* **2002**, *42*, 733.
19. Ashori, A.; Nourbakhsh, A. *Compos. B* **2010**, *41*, 578.
20. Dikobe, D. G.; Luyt, A. S. J. *Appl. Polym. Sci.* **2007**, *103*, 3645.
21. Balkan, O.; Ezdeşir, A.; Demirer, H. *Polym. Comp.* **2010**, *31*, 1265.
22. Zhou, X. P.; Li, R. K.; Xie, X. L.; Tjong, S. C. J. *Appl. Polym. Sci.* **2003**, *88*, 1055.
23. Qiu, W.; Zhang, F.; Endo, T.; Hirotsu, T. J. *Appl. Polym. Sci.* **2003**, *87*, 337.
24. Amash, A.; Zugenmaier, P.; *Polymer* **2000**, *41*, 1589.
25. Cheng, H.; Tian, M.; Zhang, L. J. *Appl. Polym. Sci.* **2008**, *109*, 2795.
26. Roy, S. B.; Ramaraj, B.; Shit, S. C.; Nayak, S. K. J. *Appl. Polym. Sci.* **2011**, *120*, 3078.
27. Ibrahim, N. A.; Hashim, N.; Rahman, M. Z. A.; Yunus, W. M. Z. W. J. *Thermoplast. Comp. Mater.* **2011**, *24*, 713.
28. Wang, Y.; Yeh, F.C.; Lai, S. M.; Chan, H. C.; Shen, H. F. *Polym. Eng. Sci.* **2003**, *43*, 933.
29. Oksman, K.; Clemons, C. J. *Appl. Polym. Sci.* **1998**, *67*, 1503.
30. Clemons, C. *Compos. A* **2010**, *41*, 1559.
31. Mariano, P.:Minhaz-UI Haque, Md.; Alvarez, V. *Polymers* **2010**, *2*, 554.
32. Law, T.T.; Mohd Ishak, Z. A. J. *Appl. Polym. Sci.* **2011**, *120*, 563.
33. Ashori, A.; Nourbakhsh, A. *Waste Manage.* **2010**, *30*, 680.
34. Rezaur, R. M.; Monimul, H. M.; NazrulI. M.; Hasan, M. *Compos. A* **2009**, *40*, 511.
35. Kaci, M.; Benhamida, A.; Cimmino, S.; Silvestre, C.; Carfagna, C. *Macromol. Mater. Eng.* **2005**, *290*, 987.